Available online at www.sciencedirect.com
ScienceDirect
Trans. Nonferrous Met. Soc. China 32(2022) 1664−1676
Transactions of Nonferrous Metals Society of China
www.tnmsc.cn

Phase conversion and removal of impurities during oxygen-rich alkali conversion of high titanium slag

Qin-qin SUI[1,2], Zhi-he DOU[1,2], Ting-an ZHANG[1,2]

1. School of Metallurgy, Northeastern University, Shenyang 110819, China;
2. Key Laboratory of Ecological Metallurgy of Multi-metal Intergrown Ores of Ministry of Education, Northeastern University, Shenyang 110819, China

Received 17 March 2021; accepted 13 September 2021

Abstract: In order to achieve high-efficiency alkali conversion and impurity removal of high titanium slag under the condition of low alkali concentration, a new way of oxygen-rich alkali conversion in KOH solution was proposed. The conversion law of element occurrence state and the influence of the conversion conditions on the titanium conversion rate and removal rate of silicon and aluminum were studied. The results showed that the KOH solution converted the titanium oxide in high titanium slag into whisker-like potassium titanate. Silicon and aluminum elements were dissolved into the solution. Under the following conditions, KOH concentration of 6 mol/L, conversion temperature of 260 °C, initial oxygen partial pressure of 2 MPa, liquid−solid ratio of 35 mL/g, conversion time of 4 h, and high titanium slag particle size of 48−74 μm, the conversion rate of titanium was 97.0%, and the removal rates of silicon and aluminum were 90.2% and 76.2%, respectively. Oxygen-rich alkali conversion product was converted to rutile with a TiO_2 grade of 99.1% by acid hydrolysis conversion.

Key words: high titanium slag; alkali conversion; conversion rate; removal rate

1 Introduction

Titanium dioxide, as one of the best white pigments, has been widely used in coatings, plastics, paper and other industries because of the following advantages, such as the best opacity and whiteness, along with its nontoxicity and stability [1−3]. At present, the main processes for the industrial production of titanium dioxide are still the sulfuric acid process and the chlorination process. The sulfuric acid process has a simple process flow and low requirements for raw materials. However, the product quality of sulfuric acid process is not good. Additionally, this process is not environmentally friendly due to its large waste emissions [4−7]. The products of the chlorination process are of high quality. However, this process has strict requirements on equipment materials and the grades of raw materials, especially the content of impurities [8−10].

In recent years, new processes that convert titanium raw materials to titanates and then use titanates to prepare titaniferous solutions or directly hydrolyze them to obtain titanium dioxide have received increasing interest [11−13]. Compared with the raw materials before conversion, the conversion product has better acid solubility. And dilute acid can be used in the subsequent process instead of concentrated acid to prepare titanium dioxide. This can reduce the difficulty of recycling the acidic medium and reduce waste discharge. The alkali conversion process can also remove some impurities, which provides the possibility to produce higher-quality titanium dioxide. As shown in Table 1, LIU et al [14] studied the conversion of

Corresponding author: Zhi-he DOU, Tel: +86-13940091053, E-mail: douzh@smm.neu.edu.cn
DOI: 10.1016/S1003-6326(22)65901-6

Table 1 Comparison of different alkali conversion methods

Alkali conversion medium	Titanium raw material	Optimal conditions (temperature, medium concentration, particle size)	Conversion rate under optimal conditions/%
Concentrated KOH solution [14]	Titanium concentrate	220 °C, 80 wt.% KOH, 160−180 μm	80−85
NaOH molten salt [15]	Titanium slag	475 °C, 100 wt.% NaOH, 48−58 μm	95−98
NaOH−KOH binary molten salt [16]	Titanium slag	350 °C, 50 mol.% NaOH + 50 mol.% KOH, 76−105 μm	98
NaOH solution [17]	Titanium slag	220 °C, 10 mol/kg H_2O, 51−61 μm	100

titanium concentrate in a concentrated KOH solution. The results show that temperature and particle size have a significant effect on titanium conversion. When using an 80 wt.% KOH solution to convert a titanium concentrate (particle size 160−180 μm) at 220 °C, the titanium conversion rate is 80%−85%. XUE et al [15] used the NaOH molten salt to convert titanium slag at 475 °C and with a titanium slag particle size of 48−58 μm; they found that 95%− 98% titanium could be converted. WANG et al [16] studied the conversion process of titanium slag in the NaOH−KOH binary molten salt (50 mol.% NaOH + 50 mol.% KOH). After 90 min of conversion at 350 °C and with a titanium slag particle size of 76−105 μm, the titanium conversion rate was greater than 98%. However, the existing high- concentration alkali conversion cannot guarantee the effective removal of silicon and other impurities in titanium raw materials [18]. In addition, high-concentration molten salt media have strict equipment requirements. ZHANG et al [17] studied the conversion effect of titanium slag in a NaOH solution. After 4 h of conversion at 220 °C, a NaOH concentration of 10 mol/kg H_2O, and a titanium slag particle size of 51−61 μm, the titanium conversion rate approached 100%. Additionally, the concentration of the alkaline medium used for the conversion was significantly reduced.

In order to further reduce the concentration of alkaline medium, in this work, high titanium slag was converted in an oxygen-rich atmosphere. Oxygen was used to oxidize the low-valence titanium in the high titanium slag to promote the conversion process. This method can significantly improve the conversion efficiency of titanium in low- concentration alkaline medium, and weaken the requirement for alkaline medium concentration. At the same time, the silicon and aluminum impurities in the high titanium slag can be efficiently removed. In addition, the decrease in the alkali medium concentration can also simplify the separation process between the alkali medium and the conversion product and the circulation process of the alkali medium. The alkali conversion product can be used to prepare titanium dioxide by dilute acid. The concentration of acid and alkaline medium required by the process is reduced, which provides a new way to realize the high-efficiency and clean production of titanium dioxide. In this work, the occurrence state and phase transition of titanium and impurities during the conversion of high titanium slag into potassium titanate in a potassium hydroxide solution under an oxygen-rich atmosphere were specifically studied. The effects of conversion conditions on the titanium conversion rate and the removal rates of silicon and aluminum impurities were investigated through single-factor experiments.

2 Experimental

2.1 Materials

The high titanium slag used in the experiments of this study was purchased from Fuxin Titanium Industry Company (Liaoning province, China). Both the potassium hydroxide solution and the hydrochloric acid solution used in the experiments were prepared from analytical grade reagents and deionized water, and the used oxygen was industrial grade.

2.2 Experimental procedure

The high titanium slag and KOH solution were added into the stainless steel reactor according to a certain liquid−solid ratio. Then, the temperature was raised to the set value according to the program for constant temperature conversion. After the reaction was completed, the conversion slurry was cooled to room temperature and removed for separation by suction filtration. The solid-phase

product was washed with deionized water to neutrality and then placed in a drying oven at 70 °C for 12−24 h. In an oxygen-free atmosphere, the high-titanium slag was converted for 1, 2, 3, 4 and 5 h under the conditions of KOH concentration of 6 mol/L, temperature of 260 °C, liquid−solid ratio of 40 mL/g, and particle size of 48−74 μm. A certain pressure of oxygen was introduced during the oxygen-rich alkali conversion. The specific experimental parameters are shown in Table 2.

2.3 Analysis

The alkali conversion products were dissolved at a low concentration of hydrofluoric acid. The dissolution process was carried out in a shaking table. The specific dissolution conditions were hydrofluoric acid concentration of 0.25 wt.%, temperature of 25 °C, liquid−solid ratio of 1000 mL/g, time of 12 h and rotating speed of 150 r/min. Under the same conditions, high titanium slag was dissolved as a blank. The content of titanium in the conversion products and solution was tested by inductively coupled plasma atomic emission spectroscopy (ICP-AES, Prodigy XP). The titanium conversion rate was calculated by formulas (1) and (2):

$$m_{\mathrm{L}}=\eta_{\mathrm{Ti}}m_{\mathrm{Ti}}+(1-\eta_{\mathrm{Ti}})m_{\mathrm{Ti}}a \tag{1}$$

$$a=\frac{m'_{\mathrm{L}}}{m'_{\mathrm{Ti}}}\times 100\% \tag{2}$$

where η_{Ti} is the titanium conversion rate, %; a is the titanium dissolution rate of the high titanium slag in a low concentration of hydrofluoric acid, %; m_{Ti} and m'_{Ti} are the masses of titanium in the conversion products and high titanium slag, respectively, g; m_{L} and m'_{L} are the masses of titanium in the hydrofluoric acid solution after dissolving the conversion products and high titanium slag, respectively, g.

The contents of silicon and aluminum in the conversion products were detected by X-ray fluorescence spectrometer (XRF, ZSX Primus II). The removal rates of silicon and aluminum were calculated by

$$\eta_{\mathrm{P}}=\left(1-\frac{m_{\mathrm{P}}}{m'_{\mathrm{P}}}\right)\times 100\% \tag{3}$$

where η_{P} is the removal rate of silicon or aluminum, %; m_{P} is the mass of silicon or aluminum in the conversion products, g; m'_{P} is the mass of silicon or aluminum in the high titanium slag, g.

The phase compositions of the samples were determined by X-ray diffraction (XRD, Ultima IV and D8 ADVANCE). The microscopic morphology of the samples was observed by scanning electron microscopy (SEM, SU−8010).

3 Results and discussion

3.1 Composition and phase analysis of high titanium slag

The chemical compositions of the high titanium slag with different particle sizes used in the experiments are shown in Table 3. The XRD pattern of the high titanium slag is shown in Fig. 1. Titanium element in high titanium slag mainly existed in the form of anosovite in the Ti_3O_5 and $Mg_{0.06}Ti_{2.94}O_5$ phases.

The SEM image and elemental distribution maps are shown in Fig. 2. The magnesium, aluminum and zirconium impurities were mainly dispersed in the form of solid solutions in anosovite. The silicon, iron, manganese and sulfur impurities were clearly enriched, and magnesium and aluminum in the silicon-rich region were relatively

Table 2 Conditions of experiments

Oxygen pressure/MPa	c(KOH)/(mol·L^{-1})	Temperature/°C	Time/h	Liquid−solid ratio/(mL·g^{-1})	Particle size/μm
0, 1, 2, 3, 4	8	240	2	40	48−74
2	2, 4, 6, 8, 10	240	2	40	48−74
2	6	200, 220, 240, 260, 280	2	40	48−74
2	6	260	1, 2, 3, 4, 5	40	48−74
2	6	260	4	20, 25, 30, 35, 40	48−74
2	6	260	4	25	270−550, 150−270, 106−150, 74−106, 48−74

Table 3 Chemical compositions of high titanium slag (wt.%)

Particle size/μm	Ti	Si	Al	Mn	Fe	Mg	S	Zr	V	Ca	Cr	Nb
48−74	55.0	0.58	1.27	0.73	2.54	0.88	0.76	0.31	0.19	0.12	0.49	0.07
74−106	54.5	0.51	1.03	0.63	2.54	0.77	1.35	0.32	0.20	0.09	0.47	0.07
106−150	54.6	0.51	1.01	0.64	2.87	0.75	1.18	0.32	0.21	0.08	0.48	0.07
150−270	55.2	0.52	0.91	0.72	2.59	0.83	1.35	0.32	0.20	0.08	0.49	0.07
270−550	54.3	0.55	1.20	0.73	2.43	0.76	1.14	0.31	0.19	0.10	0.51	0.07

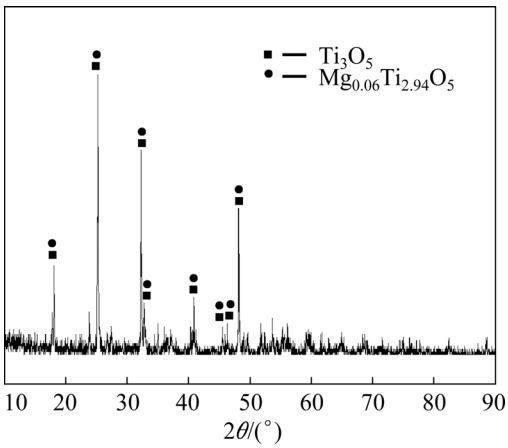

Fig. 1 XRD pattern of high titanium slag

enriched. According to the EDS microanalysis results in Table 4, the silicon impurity component in the high titanium slag was mainly in the form of free silica and existed together with impurities such as aluminum, magnesium and calcium (Spectrum 1). Iron and manganese existed mainly in the form of oxides and sulfides, and chromium components also existed in the sulfide-rich regions of iron and manganese (Spectra 3, 5 and 6). In addition, some iron and niobium coexisted (Spectrum 4), and some sulfur and carbon coexisted (Spectrum 2). Notably, the oxygen content of these two regions was low.

3.2 Influence of atmosphere on titanium conversion rate

Figure 3 shows the variation of titanium conversion rate with time under oxygen-rich and oxygen-free conditions. The overall trend of the two was similar. The titanium conversion rate increased rapidly in the early stage of conversion, and then tended to balance. However, compared with the oxygen-free condition, the titanium conversion rate under the oxygen-rich condition was increased by more than 30%. The oxygen-rich atmosphere had a significant strengthening effect on the alkali conversion process.

3.3 Titanium conversion and impurity removal during oxygen-rich alkali conversion

The effects of oxygen-rich alkali conversion conditions on the conversion rate of titanium and the removal rates of aluminum and silicon impurities were systematically studied. The phases of the conversion products under different conditions were characterized by XRD.

3.3.1 Effect of initial oxygen partial pressure

As seen from Fig. 4(a), when the initial oxygen partial pressure increased from 0 to 1 MPa, the titanium conversion rate increased from 38.4% to 54.8%, and the aluminum removal rate increased from 42.4% to 48.6%. When the initial oxygen partial pressure continued to increase to 4 MPa, the titanium conversion rate and aluminum removal rate still increased slightly. The silicon removal rate was hardly affected by the initial oxygen partial pressure. Figure 4(b) shows the XRD patterns of the alkali conversion products at different initial oxygen partial pressures. The phases of the products mainly were $K_3Ti_8O_{17}$ and $K_2Ti_8O_{17}$ phases. The characteristic peaks of $K_3Ti_8O_{17}$ and $K_2Ti_8O_{17}$ at 11.32°, 29.6° and 47.8° were more obvious. The initial oxygen partial pressure has little effect on the XRD patterns of the alkali conversion products.

The above change trends of the conversion rate of titanium and the removal rates of aluminum and silicon impurities are related to the occurrence state of elements and the law of ore-phase intercalation (Fig. 2). The titanium in the high titanium slag existed in the form of the low valence anosovite phase. The majority of aluminum was solid-dissolved in the anosovite phase, and a small amount of it was concentrated with silicon. When oxygen was present, the oxidation of low-valence titanium to high-valence titanium led to the destruction of the anosovite phase. This further promoted the conversion to potassium titanate. The reaction equations are shown in Reactions (4) and (5). LI et al [19] used ilmenite and a concentrated

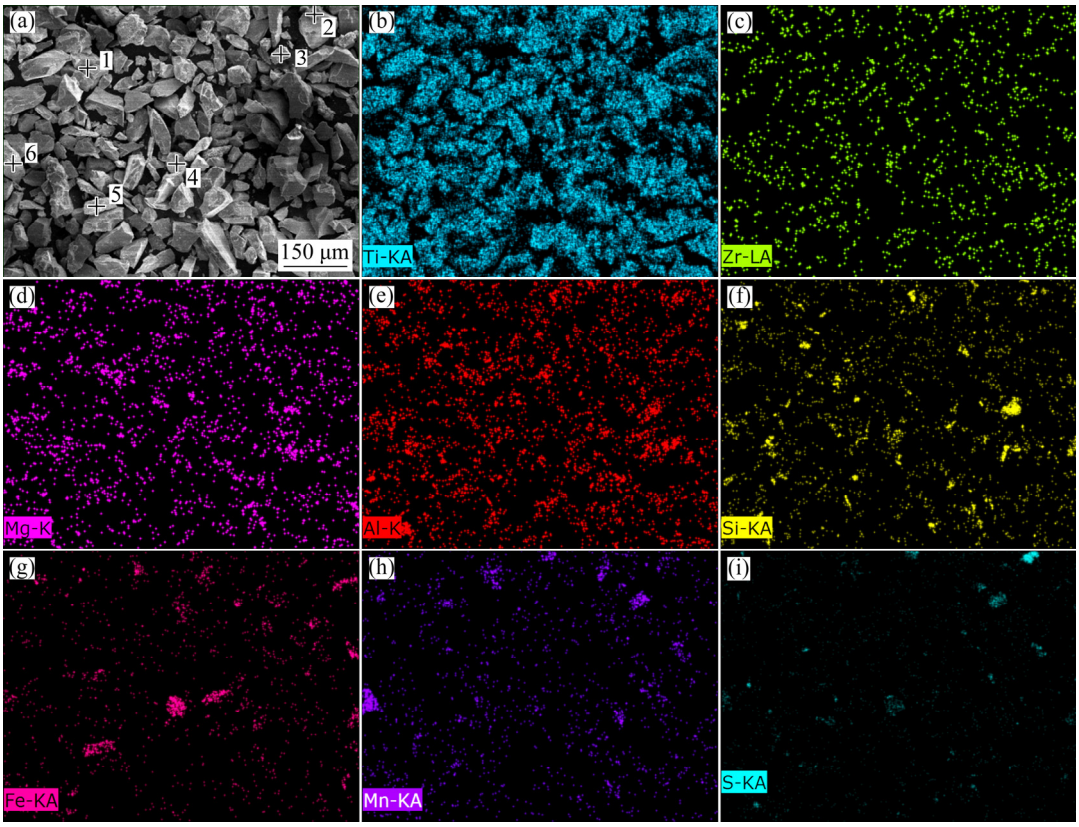

Fig. 2 SEM image (a) and elemental distribution maps (b−i) of high titanium slag

Table 4 EDS microanalysis of impurity-rich regions (wt.%)

Spot in Fig. 2(a)	C	O	S	Si	Ti	Mg	Al	Zr	Fe	Mn	V	Ca	Cr	Nb
1	4.76	54.4	0.39	18.3	5.34	2.81	7.42	0.86	0.30	1.04	0.29	1.80	0.09	–
2	24.7	4.02	68.9	0.07	0.89	0.20	0.20	0.47	–	0.06	–	–	–	–
3	4.24	23.9	26.4	–	1.40	0.31	0.06	0.03	4.53	21.9	0.59	–	16.7	–
4	7.40	11.0	3.78	3.96	2.81	0.51	0.54	0.22	41.7	0.88	0.82	–	2.56	22.5
5	2.65	38.7	–	–	9.25	0.25	0.32	–	47.1	1.41	–	0.13	0.18	–
6	2.29	37.9	2.45	–	2.48	0.30	0.04	–	1.19	47.7	–	0.07	1.91	–

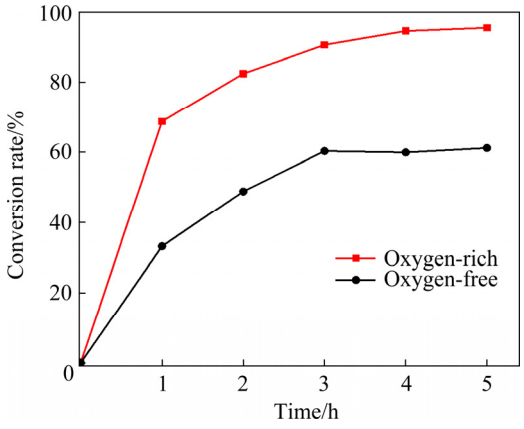

Fig. 3 Influence of atmosphere on titanium conversion rate (In an oxygen-rich atmosphere, the oxygen pressure was 2 MPa. Other experimental conditions were KOH concentration of 6 mol/L, temperature of 260 °C, liquid−solid ratio of 40 mL/g, and particle size of 48−74 μm)

potassium hydroxide solution to synthesize potassium titanate ($K_4Ti_3O_8$) in different atmospheres. The results also showed that the oxygen atmosphere was conducive to the oxidation of Fe(II) and could promote the conversion of ilmenite to potassium titanate. With the destruction of the anosovite phase, aluminum dissolved in it was released. Then, aluminum reacted with potassium hydroxide to enter the liquid phase. The silicon in the high titanium slag basically existed in a free form. It reacted directly with potassium hydroxide in the solution during the oxygen-rich alkali conversion process. The chemical reactions that may occur are shown in Reactions (6) to (10). Therefore, with the increase in initial oxygen partial pressure, the titanium conversion rate and

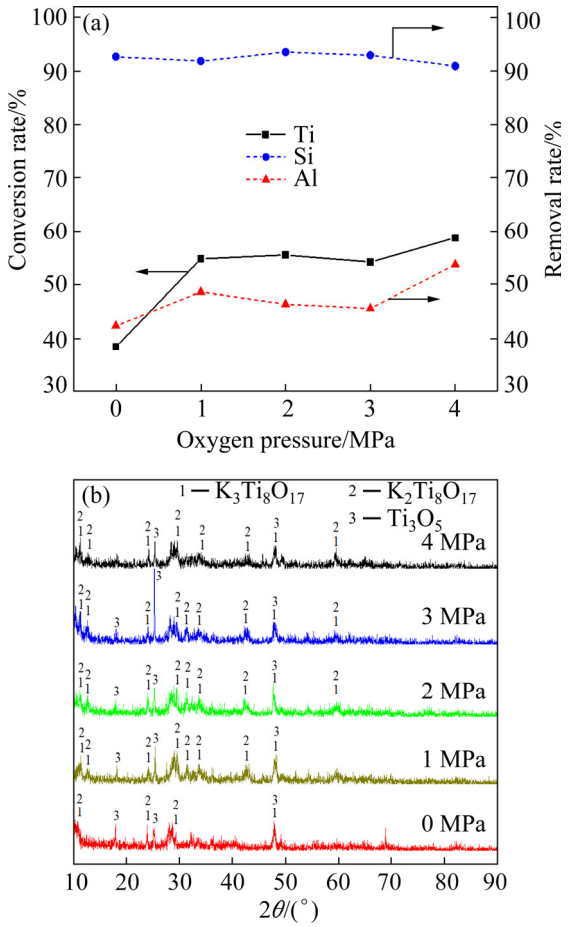

Fig. 4 Effect of initial oxygen partial pressure on conversion: (a) Conversion rate of titanium and removal rates of silicon and aluminum; (b) XRD patterns of conversion products

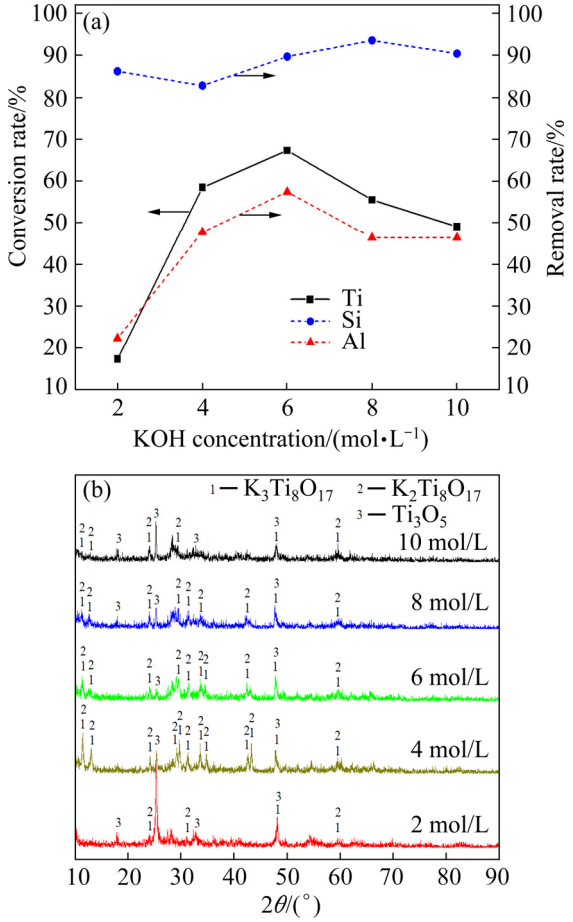

Fig. 5 Effect of KOH concentration on conversion: (a) Conversion rate of titanium and removal rate of silicon and aluminum; (b) XRD patterns of conversion products

aluminum removal rate increased, while the silicon removal rate was basically unchanged.

$$32Ti_3O_5+36KOH+13O_2\rightarrow 12K_3Ti_8O_{17}+18H_2O \quad (4)$$

$$8Ti_3O_5+6KOH+4O_2\rightarrow 3K_2Ti_8O_{17}+3H_2O \quad (5)$$

$$Al_2O_3+2OH^-\rightarrow 2AlO_2^-+H_2O \quad (6)$$

$$Al_2O_3+2OH^-+3H_2O\rightarrow 2Al(OH)_4^- \quad (7)$$

$$SiO_2+OH^-+H_2O\rightarrow SiO(OH)_3^- \quad (8)$$

$$SiO_2+2OH^-\rightarrow SiO_2(OH)_2^{2-} \quad (9)$$

$$SiO_2+3OH^-\rightarrow SiO_3(OH)^{3-}+H_2O \quad (10)$$

3.3.2 Effect of KOH concentration

As shown in Fig. 5(a), when the potassium hydroxide concentration changed from 2 to 10 mol/L, the titanium conversion rate and aluminum removal rate first increased and then decreased. When the concentration of potassium hydroxide was 6 mol/L, the titanium conversion rate and aluminum removal rate reached their highest values of 67.3% and 57.4%, respectively. The silicon removal rate increased with increasing potassium hydroxide concentration, reaching 93.5% at 8 mol/L. Since silicon was free of the titanium-rich phase, the potassium titanate product formed during the oxygen-rich alkali conversion process did not form a product layer on the surface of the silicon-rich phase. The effect of the alkali concentration on the silicon removal rate was not significant during the process of alkali conversion and impurity removal. Aluminum mostly coexisted with titanium, and potassium titanate formed by alkali conversion formed a product layer that hinders the reaction. Therefore, as the alkali concentration increased, the mass transfer resistance increased, and the aluminum removal rate and titanium conversion rate decreased. The concentration of potassium hydroxide has a

significant effect on the XRD patterns of the alkali conversion products (Fig. 5(b)). When the potassium hydroxide concentration was 4 mol/L, the characteristic peaks of potassium titanates ($K_3Ti_8O_{17}$ and $K_2Ti_8O_{17}$) at 11.32° and 12.96° were clearly stronger than those of the alkali conversion products at other concentrations. As the potassium hydroxide concentration increased from 2 to 6 mol/L, the peak intensity of the Ti_3O_5 phase in the conversion products at 25.17° became significantly weaker. However, after further increasing the potassium hydroxide concentration, the peak intensity of the Ti_3O_5 phase was enhanced. JIN et al [20] and YAN et al [21] reported that as the concentration of potassium hydroxide increased, the solubility of oxygen decreased rapidly, and the viscosity of the solution increased. This increase in viscosity reduced the diffusion coefficient of dissolved oxygen, which in turn affected the redox process in the solution. According to Reactions (4) and (5), the increase in the potassium hydroxide concentration was favorable for the conversion reaction to proceed to the right. However, its effect on oxygen dissolution and diffusion was not conducive to the destruction of the anosovite phase (Ti_3O_5) by oxidation.

3.3.3 Effect of conversion temperature

With increasing conversion temperature, the titanium conversion rate and aluminum removal rate increased significantly (Fig. 6(a)). When the alkali conversion temperature increased to 280 °C, the titanium conversion rate reached 86.5%, and the aluminum removal rate reached 75.1%. The silicon removal rate was always maintained above 88.0%. As the temperature increased, the characteristic peaks of the Ti_3O_5 phase in the XRD patterns of the alkali conversion products gradually weakened, and the characteristic peaks of the potassium titanate phase increased significantly (Fig. 6(b)).

3.3.4 Effect of conversion time

The titanium conversion rate and aluminum removal rate increased rapidly over time and then equilibrated (Fig. 7(a)). After 4 h of oxygen-rich alkali conversion, the titanium conversion rate reached more than 94.0%, and the aluminum removal rate reached 76.2%. The silicon removal rate was maintained at approximately 90.0%. The characteristic peaks of $K_3Ti_8O_{17}$ and $K_2Ti_8O_{17}$ in the XRD patterns of the products also gradually increased with increasing conversion time (Fig. 7(b)).

3.3.5 Effect of liquid−solid ratio

When the liquid−solid ratio was greater than 20 mL/g, the effect of the liquid−solid ratio on the oxygen-rich alkali conversion was not obvious (Fig. 8). However, when the liquid−solid ratio was less than 20 mL/g, the solid phase agglomerated on the inner wall of the reactor near the liquid level during the alkali conversion process. This affected the contact between the solid and liquid phases and worsened the effect of alkali conversion.

3.3.6 Effect of particle size

As shown in Fig. 9, the particle size of the high titanium slag had a significant effect on the conversion rate of titanium and removal rate of aluminum. As the particle size decreased, the conversion rate of titanium and removal rate of aluminum increased rapidly. The characteristic

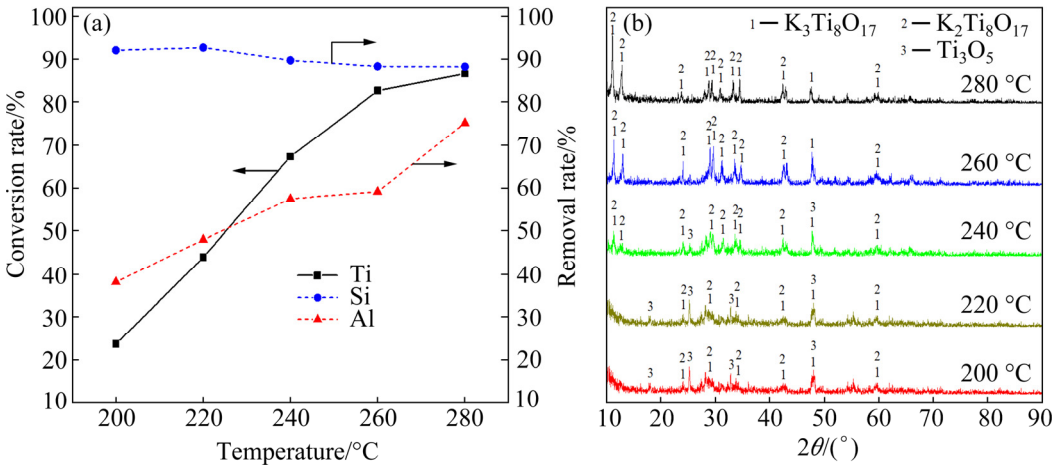

Fig. 6 Effect of temperature on conversion: (a) Conversion rate of titanium and removal rates of silicon and aluminum; (b) XRD patterns of conversion products

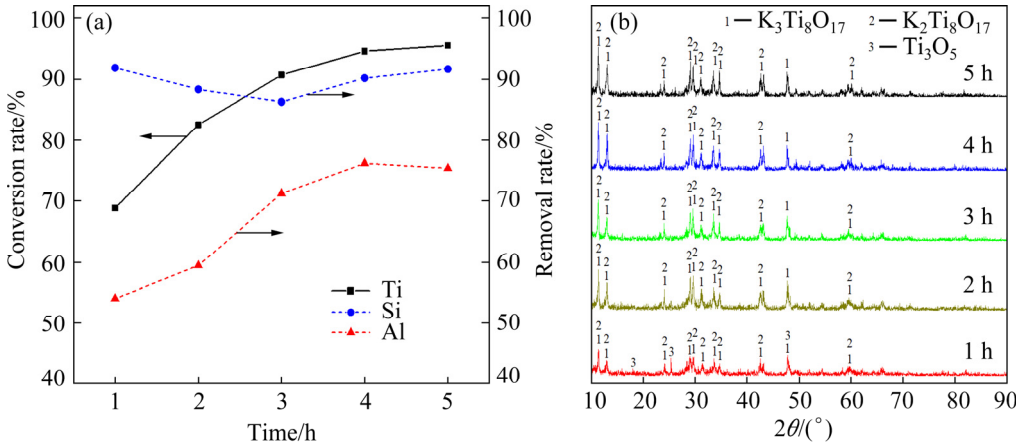

Fig. 7 Effect of time on conversion: (a) Conversion rate of titanium and removal rates of silicon and aluminum; (b) XRD patterns of conversion products

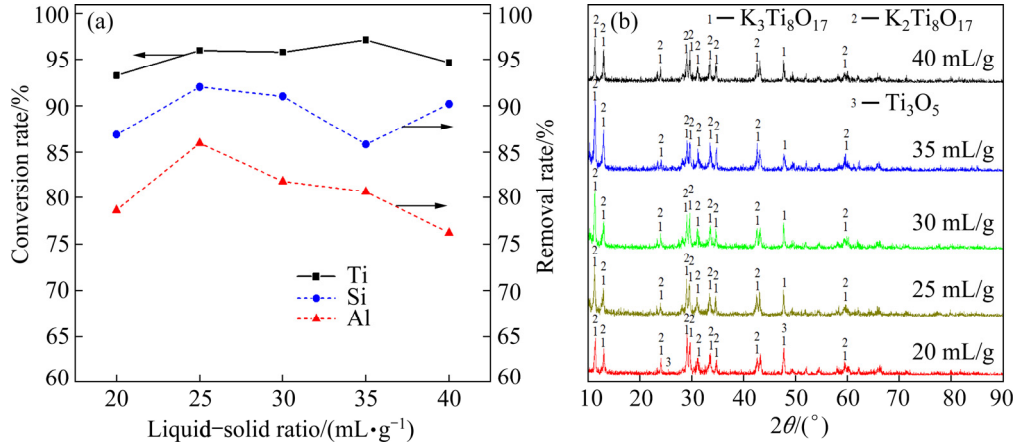

Fig. 8 Effect of liquid−solid ratio on conversion: (a) Conversion rate of titanium and removal rates of silicon and aluminum; (b) XRD patterns of conversion products

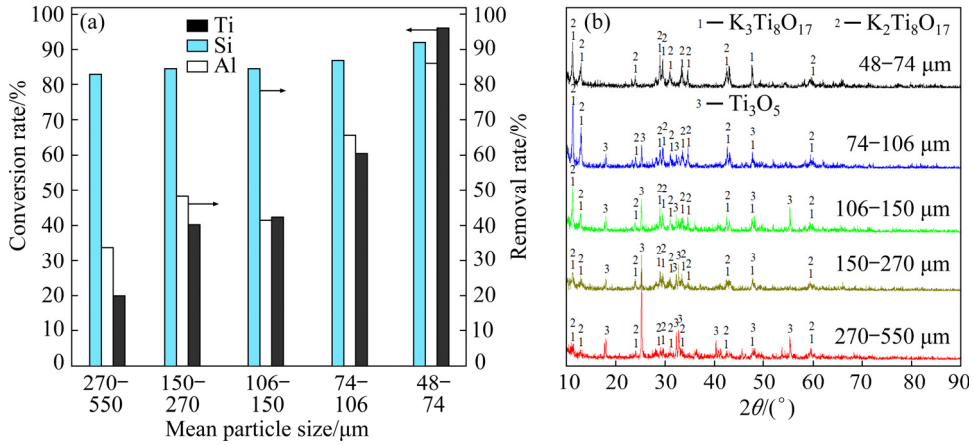

Fig. 9 Effect of particle size on conversion: (a) Conversion rate of titanium and removal rates of silicon and aluminum; (b) XRD patterns of conversion products

peaks of the potassium titanate phase in the XRD patterns of the products also gradually increased. The removal rate of silicon impurities varied slightly.

3.4 Law of transition of different constituents in process of oxygen-rich alkali conversion

Figures 10 and 11 show the SEM images and elemental distribution maps of the oxygen-rich

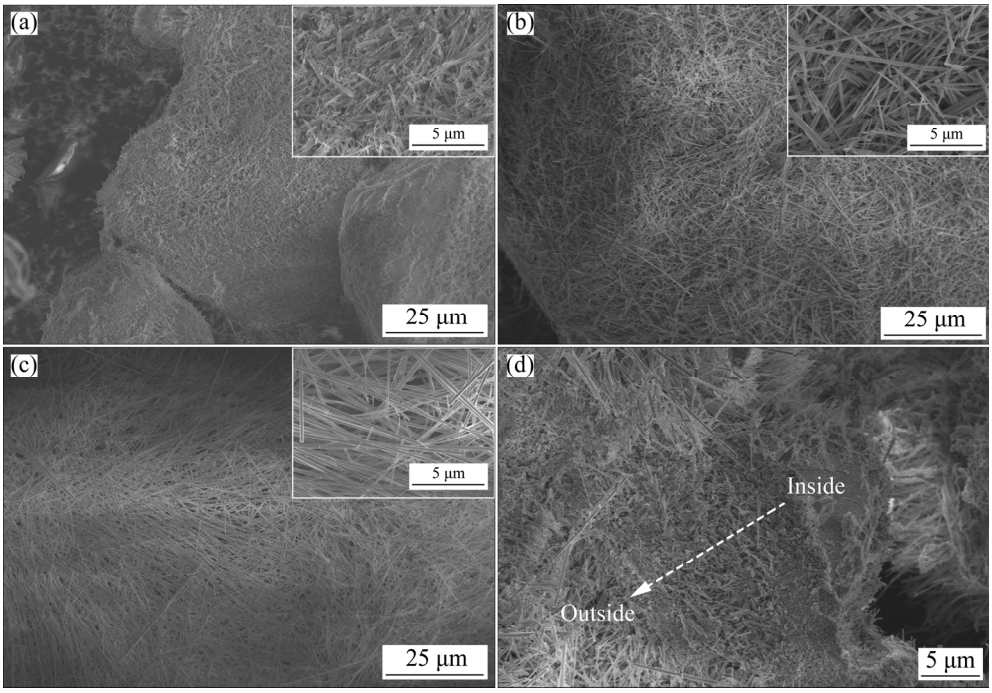

Fig. 10 SEM images of conversion product: (a) Conversion at 200 °C for 2 h; (b) Conversion at 240 °C for 2 h; (c, d) Conversion at 260 °C for 1 h (KOH concentration of 6 mol/L, oxygen pressure of 2 MPa, liquid−solid ratio of 40 mL/g, and particle size of 48−74 μm)

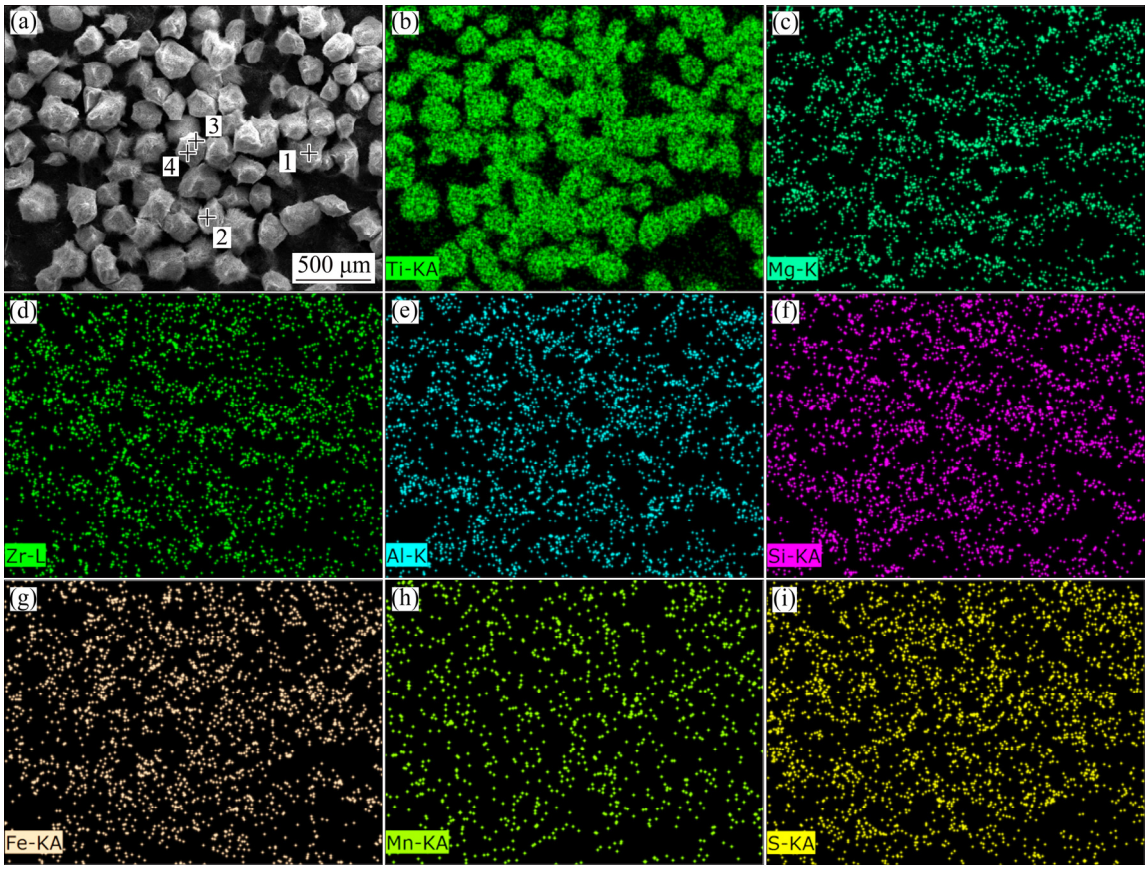

Fig. 11 SEM image (a) and elemental distribution maps (b−i) of conversion product (KOH concentration of 6 mol/L, oxygen pressure of 2 MPa, temperature of 260 °C, time of 4 h, liquid−solid ratio of 25 mL/g, and particle size of 48−74 μm)

alkali conversion products, respectively. As seen from Figs. 10 and 11, after the high titanium slag was alkali-converted, the titanium-containing phase changed from smooth and dense particles mainly consisting of anosovite to agglomerates that are nearly spherical. Further observation of the near-spherical agglomerates in Fig. 11 showed that the agglomerates were formed by a large number of whiskers or rod-shaped crystals. From the SEM images of the alkali conversion products shown in Fig. 10, as the alkali conversion temperature increased, the diameter and length of these alkali conversion product whiskers increased significantly, and the product layer formed by the conversion product became loose. When alkali conversion was performed at 200 °C for 2 h, the conversion products were mainly composed of fine whiskers and nanowires (Fig. 10(a)). When converted at 240 °C for 2 h, the nanowires in the conversion product were greatly reduced, and whiskers with high aspect ratios were formed (Fig. 10(b)). As the conversion temperature increased, the whiskers developed more completely (Fig. 10(c)).

To analyze the internal structure of the conversion product, it was rolled with a toothpick tip to peel off the product layer, as shown in Fig. 10(d). After the whisker-like product layer of the sample converted at 260 °C for 1 h was peeled off, the unconverted titanium slag particles wrapped by the product were exposed. XIE et al [22] believed that in an alkaline solution under hydrothermal conditions, titanium of various titanium-containing precursors was dissolved under the action of hydroxide ions. After supersaturation, nucleation occurred to generate titanate crystals. At the same time, DU et al [23] studied the process of generating potassium titanate through the reaction of titanium dioxide and potassium hydroxide solution. The results showed that potassium titanate crystal nuclei were first formed on the surface of titanium dioxide particles and continued to grow on the surface over time. Figure 10(d) shows that from the inside to the outside of the potassium titanate product layer, the crystal size gradually increased, and the whisker developed more complete. Furthermore, small potassium titanate crystal grains only existed on the surface of the high titanium slag particles. This shows that, similar to the research of DU et al [23], after the titanium-containing phase (Ti_3O_5) in the high titanium slag was decomposed, the dissolved titanium nucleated on the surface of the high titanium slag to form potassium titanate crystals. This can also be explained by the fact that heterogeneous nucleation requires a lower concentration than homogeneous nucleation [24,25].

The elemental distribution maps are shown in Fig. 11. The impurities, magnesium, aluminum and zirconium, were still spread-out in the conversion product. However, the distribution of the silicon, iron, manganese and sulfur enrichment in high titanium slag changed significantly. They had not significant enrichment in the conversion products. It is known from Table 5 that the relative content of silicon and sulfur in the slag after alkali conversion significantly decreased, indicating that they were effectively dissolved in the liquid phase. Free silica was converted to soluble silicate, and low-valence sulfur was oxidized to sulfate under the action of oxygen. Magnesium, zirconium, iron and calcium impurities were difficult to remove by alkali conversion because they could enter the potassium titanate lattice by substitution. A part of aluminum and manganese were leached and the others entered into the potassium titanate product by substitution. Moreover, there was a small amount of common enrichment of iron, manganese and chromium, which may be due to the common enrichment of these three elements as sulfides in high titanium slag. The concentrations of iron, manganese and chromium in the enriched region during the alkali conversion process were higher. And they were still relatively enriched after being substituted into potassium titanate crystals [17].

Table 5 EDS microanalysis of conversion products (wt.%)

Spot in Fig. 11(a)	C	O	K	Ti	Si	S	Mg	Al	Ca	V	Cr	Mn	Fe	Zr
1	1.59	34.7	14.2	47.7	0.04	−	0.33	0.25	0.32	0.10	−	−	0.64	0.15
2	2.00	34.0	13.4	49.1	−	−	0.43	0.24	0.23	0.11	−	−	0.38	0.06
3	2.00	40.7	13.0	40.4	−	−	0.23	0.21	0.31	−	0.13	0.23	2.80	0.04
4	2.45	26.3	13.4	53.0	−	0.02	0.40	0.40	0.16	−	0.30	0.52	2.80	0.29

3.5 Acid hydrolysis conversion of alkali conversion product

According to the phase analysis results of the alkali conversion products, titanium oxide was converted into the $K_3Ti_8O_{17}$ and $K_2Ti_8O_{17}$ phases during the oxygen-rich alkali conversion process. Most of the silicon and aluminum impurities were dissolved into the liquid phase and removed. Impurities such as magnesium, zirconium and iron entered the potassium titanate crystal lattice by substitution. To obtain high-purity titanium dioxide, it is necessary to further convert the alkali conversion products by acid hydrolysis. After reacting at a temperature of 260 °C, an oxygen partial pressure of 1 MPa, and a KOH concentration of 6 mol/L for 10 h, an alkali conversion product was obtained. Then, it was subjected to acid hydrolysis for 4 h at a temperature of 130 °C, a hydrochloric acid concentration of 15 wt.% and a liquid−solid ratio of 25 mL/g to obtain an acid hydrolysis conversion product. The XRD pattern and SEM image of the acid hydrolysis conversion product are shown in Fig. 12. Its phase was rutile TiO_2, and its morphology was the short rod-like crystal with a diameter and length of approximately 200 and 800 nm, respectively. Additionally, some of these short rod-like crystals self-assembled into dendritic or flower-like shapes. Figure 13 shows the XRD pattern and SEM image of the acid hydrolysis conversion product after being calcined at 850 °C for 2 h. The calcined product was still rutile TiO_2. Compared with that before calcination (Fig. 12(a)), the full width at half maximum of the characteristic peak of the TiO_2 phase was greatly reduced, and the peak intensity was significantly enhanced. The fine crystals in the product decreased, and the overall appearance did not change much (Fig. 13(b)). XRF analysis showed that the calcined product had a TiO_2 grade of 99.1%, and iron impurities were further removed (TFe 0.03%). However, zirconium impurities were enriched (ZrO_2 0.43%).

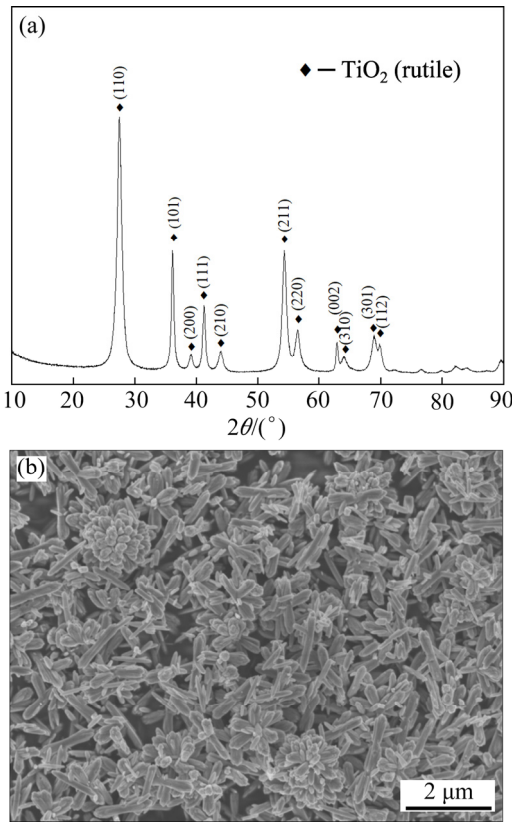

Fig. 12 XRD pattern (a) and SEM image (b) of acid hydrolysis conversion product

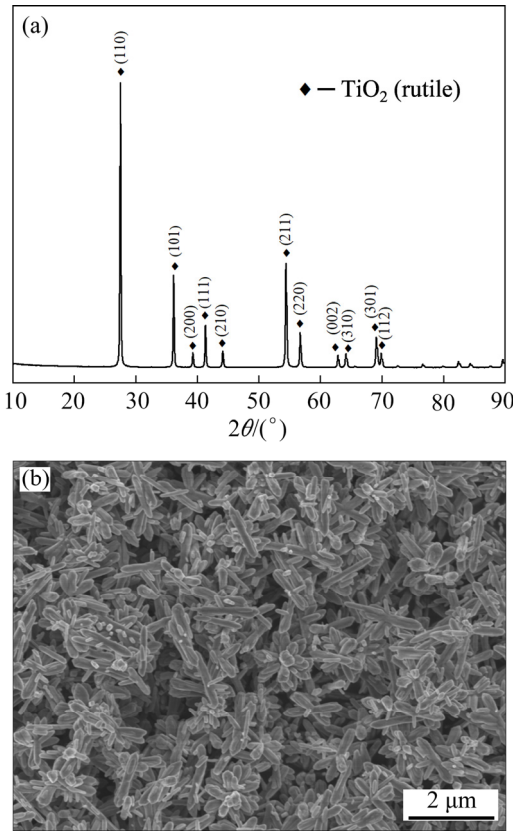

Fig. 13 XRD pattern (a) and SEM image (b) of calcined product

4 Conclusions

(1) The oxygen-rich atmosphere significantly increased the titanium conversion rate.

(2) The potassium hydroxide solution converted titanium oxide into whisker-like potassium titanate. And silicon and aluminum elements were dissolved into the solution.

(3) Under the following conversion conditions, potassium hydroxide concentration of 6 mol/L, conversion temperature of 260 °C, oxygen partial pressure of 2 MPa, liquid−solid ratio of 35 mL/g, conversion time of 4 h, and high titanium slag particle size of 48−74 μm, the conversion rate of titanium was 97.0%, and the removal rates of silicon and aluminum were 90.2% and 76.2%, respectively.

(4) After the alkali conversion product was subjected to acid hydrolysis conversion and calcination, rutile with a TiO_2 grade of 99.1% was obtained.

Acknowledgments

This work was supported by the National Natural Science Foundation of China (Nos. U1908225, U1702253), and Fundamental Research Funds for the Central Universities of China (Nos. N182515007, N170908001, N2025004).

References

[1] ZHANG Wen-sheng, ZHU Zhao-wu, CHENG Chu-yong. A literature review of titanium metallurgical processes [J]. Hydrometallurgy, 2011, 108: 177−188.

[2] LIU Wei-zao, LÜ Li, YUE Hai-rong, LIANG Bin, LI Chun. Combined production of synthetic rutile in the sulfate TiO_2 process [J]. Journal of Alloys and Compounds, 2017, 705: 572−580.

[3] LIANG Yu, DING Hao. Mineral-TiO_2 composites: Preparation and application in papermaking, paints and plastics [J]. Journal of Alloys and Compounds, 2020, 844: 156139.

[4] LI Chun, LIANG Bin, GUO Ling-hong. Dissolution of mechanically activated Panzhihua ilmenites in dilute solutions of sulphuric acid [J]. Hydrometallurgy, 2007, 89: 1−10.

[5] SACHKOV V, NEFEDOV R, ORLOV V, MEDVEDEV R, SACHKOVA A. Hydrometallurgical processing technology of titanomagnetite ores [J]. Minerals, 2017, 8: 2.

[6] GÁZQUEZ M J, BOLÍVAR J P, GARCÍA-TENORIO R, VACA F. Physicochemical characterization of raw materials and co-products from the titanium dioxide industry [J]. Journal of Hazardous Materials, 2009, 166: 1429−1440.

[7] CONTRERAS M, GÁZQUEZ M J, PÉREZ-MORENO S M, ROMERO M, BOLÍVAR J P. Management and valorisation of wastes and co-products from the TiO_2 pigment industry [J]. Waste and Biomass Valorization, 2016, 7: 899−912.

[8] YANG F L, HLAVACEK V. Effective extraction of titanium from rutile by a low-temperature chloride process [J]. AIChE Journal, 2000, 46: 355−360.

[9] ZHENG Fu-qiang, GUO Yu-feng, LIU Shui-shi, QIU Guan-zhou, CHEN Feng, JIANG Tao, WANG Shuai. Removal of magnesium and calcium from electric furnace titanium slag by H_3PO_4 oxidation roasting-leaching process [J]. Transactions of Nonferrous Metals Society of China, 2018, 28: 356−366.

[10] HAN Ji-qing, ZHANG Jia-hao, CHEN Xiao, ZHANG Jing, ZHANG Li, TU Gan-feng. Effect of rutile crystal shapes on its settlement [J]. Transactions of Nonferrous Metals Society of China, 2020, 30: 2848−2860.

[11] SANCHEZ-SEGADO S, MAKANYIRE T, ESCUDERO-CASTEJON L, HARA Y, JHA A. Reclamation of reactive metal oxides from complex minerals using alkali roasting and leaching—An improved approach to process engineering [J]. Green Chemistry, 2015, 17: 2059−2080.

[12] NGUYEN T H, LEE M S. A review on the recovery of titanium dioxide from ilmenite ores by direct leaching technologies [J]. Mineral Processing and Extractive Metallurgy Review, 2019, 40: 231−247.

[13] YU Zhi-gang, XIAO Jing-wu, LENG Hai-yan, CHOU Kuo-chih. Direct carbothermic reduction of ilmenite concentrates by adding high dosage of Na_2CO_3 in microwave field [J]. Transactions of Nonferrous Metals Society of China, 2021, 31: 1818−1827

[14] LIU Yu-min, QI Tao, CHU Jing-long, TONG Qi-jie, ZHANG Yi. Decomposition of ilmenite by concentrated KOH solution under atmospheric pressure [J]. International Journal of Mineral Processing, 2006, 81: 79−84.

[15] XUE Tian-yan, WANG Li-na, QI Tao, CHU Jing-long, LIU Chang-hou. Decomposition kinetics of titanium slag in sodium hydroxide system [J]. Hydrometallurgy, 2009, 95: 22−27.

[16] WANG Dong, CHU Jing-long, LIU Ya-hui, LI Jie, XUE Tian-yan, WANG Wei-jing, QI Tao. Novel process for titanium dioxide production from titanium slag: NaOH−KOH binary molten salt roasting and water leaching [J]. Industrial & Engineering Chemistry Research, 2013, 52: 15756−15762.

[17] ZHANG Yong-jie, QI Tao, ZHANG Yi. A novel preparation of titanium dioxide from titanium slag [J]. Hydrometallurgy, 2009, 96: 52−56.

[18] LIU Yu-min, LÜ Hua, QI Tao, ZHANG Yi. Extraction behaviours of titanium and other impurities in the decomposition process of ilmenite by highly concentrated KOH solution [J]. International Journal of Minerals, Metallurgy and Materials, 2012, 19: 9−14.

[19] LI Jie, WANG Yong, WANG Li-na, SUN Ti-chang, QI Tao, ZHANG Yi. Effect of atmosphere on the synthesis of potassium titanate [J]. Rare Metals, 2010, 29: 280−285.

[20] JIN Wei, DU Hao, ZHENG Shi-li, XU Hong-bin, ZHANG Yi. Comparison of the oxygen reduction reaction between NaOH and KOH solutions on a Pt electrode: The electrolyte-dependent effect [J]. The Journal of Physical Chemistry B, 2010, 114: 6542−6548.

[21] YAN Wen-yi, ZHENG Shi-li, JIN Wei, PENG Zhong, WANG Shao-na, DU Hao, ZHANG Yi. The influence of KOH concentration, oxygen partial pressure and temperature on the oxygen reduction reaction at Pt electrodes [J]. Journal of Electroanalytical Chemistry, 2015, 741: 100−108.

[22] XIE Jie, WANG Xiao-hui, ZHOU Yan-chun. Understanding formation mechanism of titanate nanowires through

hydrothermal treatment of various Ti-containing precursors in basic solutions [J]. Journal of Materials Science & Technology, 2012, 28: 488−494.

[23] DU G H, CHEN Q, HAN P D, YU Y, PENG L M. Potassium titanate nanowires: Structure, growth, and optical properties [J]. Physical Review B, 2003, 67: 035323.

[24] LI Wei, YANG Jian-ping, WU Zhang-xiong, WANG Jin-xiu, LI Bin, FENG Shan-shan, DENG Yong-hui, ZHANG Fan, ZHAO Dong-yuan. A versatile kinetics-controlled coating method to construct uniform porous TiO_2 shells for multifunctional core-shell structures [J]. Journal of the American Chemical Society, 2012, 134: 11864−11867.

[25] LI Wei, ZHAO Dong-yuan. Extension of the Stöber method to construct mesoporous SiO_2 and TiO_2 shells for uniform multifunctional core-shell structures [J]. Advanced Materials, 2013, 25: 142−149.

高钛渣富氧碱转化过程中物相转化与杂质脱除

随钦钦[1,2]，豆志河[1,2]，张廷安[1,2]

1. 东北大学 冶金学院，沈阳 110819；
2. 东北大学 多金属共生矿生态冶金教育部重点实验室，沈阳 110819

摘　要：为了实现低碱浓度下高钛渣的高效碱转化和除杂，提出在氢氧化钾溶液中富氧碱转化的新途径。研究富氧碱转化过程中各元素赋存状态转化规律以及转化条件对钛转化率及硅铝杂质去除率的影响规律。结果表明：氢氧化钾溶液将高钛渣中钛氧化物转化为晶须状钛酸钾，硅和铝元素溶解进入溶液；当氢氧化钾浓度为 6 mol/L，转化温度为 260 °C，初始氧分压为 2 MPa，液固比为 35 mL/g，转化时间为 4 h，高钛渣粒度为 48−74 μm 时，高钛渣中钛氧化物的转化率为 97.0%，硅铝去除率分别为 90.2%和 76.2%。富氧碱转化产物经酸解转化可得到 TiO_2 品位为 99.1%的金红石。

关键词：高钛渣；碱转化；转化率；脱除率

(Edited by Xiang-qun LI)